Two-layer Adaptive Funnel MRAC with Applications to the Control of Multi-Rotor UAVs

Mattia Gramuglia[1], Giri M. Kumar[1], and Andrea L'Afflitto[2]

***Abstract*— This paper merges for the first time two recent forms of adaptive control techniques, namely two-layer model reference adaptive control (MRAC) and funnel control, also known as tube-based control. Two-layer MRAC allows the user to set the rate of convergence of the tracking error arbitrarily high without altering the user-defined reference model or relying on barrier functions. Funnel control is a technique whereby the tracking error is constrained within bounds that can be progressively tighter. The proposed approach merges the benefits of both techniques and, for the first time in the literature on funnel control, explicitly regulates the diameter of the funnel through some user-defined adaptive law. The proposed results are tested by simulating payload delivery missions using multi-rotor unmanned aerial vehicles (UAVs) in the high-fidelity environment PyChrono.**

***Index Terms*— Adaptive control, Funnel control, Multi-rotor UAVs.**

I. Introduction

This paper presents a novel model reference adaptive control (MRAC) system, named *two-layer adaptive funnel MRAC*. This control system assures asymptotic convergence of the trajectory tracking error to zero at a user-defined rate of convergence, despite parametric and matched functional uncertainties, while meeting user-defined bounds on the tracking error. The bounds on the tracking error are set as solutions of an adaptive system that meets user-defined performance criteria. The rate of convergence of the tracking error is not necessarily enforced by the rate at which the diameter of the funnel decreases as it occurs in alternative control systems. Furthermore, the proposed results are obtained without modifying the user-defined reference model or reference command input.

MRAC systems allow to steer the trajectories of plants affected by parametric and matched functional uncertainties toward the trajectory of a user-defined reference model. One of the limitations of classical MRAC systems lies in that the controlled plant trajectory reaches the reference trajectory after the reference model's transient has decayed, and, hence, the closed-loop plant misses some of the desirable properties of the reference model. Barrier Lyapunov functions have been employed to impose user-defined constraints on the trajectory tracking error, and enforce user-defined rates of convergence [1]. If not carefully tuned, this ingenious approach, however, may imply large control efforts, especially in the case of tight bounds. Two-layer model reference adaptive control allows imposing the rate of convergence of the tracking error without employing barrier Lyapunov functions. Indeed, this result is obtained by introducing an additional reference model, which is primarily effective in the transient stage, and by adding a term to the classical MRAC law, which accounts for the trajectory tracking error. Additional details on the advantages of two-layer MRAC over alternative systems to enforce the closed-loop system's rate of convergence are discussed in detail in [2]. By itself, however, two-layer MRAC is unable to enforce user-defined bounds on the trajectory tracking error.

Funnel control [3], also known as tube control, is a class of techniques aimed at imposing user-defined bounds on the trajectory tracking error that are defined according to some user-defined criteria. Leveraging the notion of goal adaptation [4], the idea of funnel control has been ported to the MRAC framework in [5]–[7]. This framework allows to impose user-defined performance criteria by modifying the reference command input, that is, the user-defined input to the reference model. While this approach has been proven valuable as it allows merging optimal control with MRAC design, it also limits the user's freedom in setting the reference trajectory. Indeed, the reference command input is to be interpreted as the user's input to the ideal closed-loop plant's model captured by the reference model.

The results presented in this paper advance the state of the art because they allows setting variable bounds on the trajectory tracking error, as it occurs in funnel control, and also allows setting the rate of convergence of the tracking error without having to impose a rate of convergence on the diameter of the funnel, wherein the tracking error must lie. Therefore, in two-layer adaptive funnel MRAC, the role of the funnel is to certify that some bounds on the tracking error are met, while the rate of convergence of the tracking error is enforced by means of the two-layer technology. This approach allows preventing large control efforts usually associated with the use of barrier functions. Furthermore, the proposed approach does not require to modify the user-defined reference model or reference command input.

A unique feature of the proposed two-layer adaptive funnel MRAC system is that the diameter of the funnel, that is, the bounds on the trajectory tracking error, can be imposed either *a priori*, as it occurs in several current systems [1], or adaptively. Specifically, the diameter of the funnel can be automatically regulated to meet some user-defined criteria. To illustrate this notion, in this paper, we consider the problem of imposing soft constraint on the saturation of the control input. In this case, if the norm of the control

[1]M. Gramuglia and G. M. Kumar are with Virginia Tech, Department of Mechanical Engineering, Blacksburg, VA 24061, USA

[2]Andrea L'Afflitto is with the Department of Industrial and Systems Engineering of Virginia Tech, Blacksburg, VA, USA (email: a.lafflitto@vt.edu)

input is far from the user-defined saturation bounds, then the diameter of the funnel decreases. Alternatively, if the norm of the control input approaches the saturation limit, then the diameter of the funnel becomes larger, within user-defined bounds.

The effectiveness of the proposed results are proven through high-fidelity numerical simulations. In particular, we consider the problem of regulating the dynamics of an X8-copter transporting an unknown payload whose mass is approximately half of the mass of the UAV (unmanned aerial vehicle) and that is free to move within its casing. An X8-copter has been considered because it allows to produce larger thrust than quadcopters of the same dimensions and equipped with the same motor/propeller combination. Over the course of its mission, the UAV experiences several challenges that include the deactivation of one of the motors, the malfunctioning of an additional motor, and the unexpected dropping of the payload. These results have been obtained exploiting the simulation environment PyChrono, wherein a highly detailed CAD (computer aided design) model of an actual X8-copter has been imported. It is apparent how the two-layer adaptive funnel MRAC system outperforms a classical MRAC architecture and a two-layer MRAC architecture.

This paper is structured as follows. In Section II, we formally state the problem pursued in this paper. Successively, Section III recalls the fundamentals of two-layer MRAC. Section IV presents the key original result of this paper, namely two-layer adaptive funnel MRAC system. Sections V details how the proposed adaptive control architecture can be applied to control UAVs, and Section VI presents the results of high-fidelity numerical simulations obtained by employing Project Chrono [8] as the physics engine. Finally, Section VII draws conclusions on this work.

II. Problem Statement

The problem considered in this paper can be formulated as follows. Consider the plant model

$$\dot{x}(t) = Ax(t) + B\Lambda\left[u(t) + \Theta^{\mathrm{T}}\Phi(t, x(t))\right], \quad x(t_0) = x_0, \quad t \geq t_0, \tag{1}$$

where $x : [t_0, \infty) \to \mathbb{R}^n$ denotes the *plant state*, $u : [t_0, \infty) \to \mathbb{R}^m$ denotes the *control input*, $\Phi : [t_0, \infty) \times \mathbb{R}^n \to \mathbb{R}^N$ denotes the *regressor vector*, $A \in \mathbb{R}^{n\times n}$ is unknown, $B \in \mathbb{R}^{n\times m}$ is known and such that the pair $(A, B\Lambda)$ is controllable, $\Lambda \in \mathbb{R}^{m\times m}$ is diagonal, positive-definite, and unknown, and $\Theta \in \mathbb{R}^{N\times m}$ is unknown and such that $\Theta^{\mathrm{T}}\Phi(t, x)$ captures matched uncertainties for all $(t, x) \in [t_0, \infty) \times \mathbb{R}^n$. Our goal is to design an adaptive control system such that the plant trajectory $x(\cdot)$ follows the trajectory of the *reference model*

$$\dot{x}_{\mathrm{ref}}(t) = A_{\mathrm{ref}}x_{\mathrm{ref}}(t) + B_{\mathrm{ref}}r(t), \quad x_{\mathrm{ref}}(t_0) = x_{\mathrm{ref},0}, \quad t \geq t_0, \tag{2}$$

where $x_{\mathrm{ref}} : [t_0, \infty) \to \mathbb{R}^n$ denotes the *reference trajectory*, $r : [t_0, \infty) \to \mathbb{R}^m$ is user-defined, continuous, uniformly bounded, and denotes the *reference command input*, $A_{\mathrm{ref}} \in \mathbb{R}^{n\times n}$ is user-defined Hurwitz, $B_{\mathrm{ref}} \in \mathbb{R}^{n\times m}$ is user-defined, and the matching conditions

$$A_{\mathrm{ref}} = A + B\Lambda K_x^{\mathrm{T}}, \quad B_{\mathrm{ref}} = B\Lambda K_r^{\mathrm{T}} \tag{3}$$

are verified by some $K_x \in \mathbb{R}^{n\times n}$ and $K_r \in \mathbb{R}^{n\times m}$. Our first goal is to find an adaptive law such that $\lim_{t\to\infty} e(t) = 0$, where $e(t) \triangleq x(t) - x_{\mathrm{ref}}(t)$ denotes the *trajectory tracking error*. Our second goal is to impose that both $t \mapsto e(t)$ and $t \mapsto \hat{K}(t)$ are bounded for all $t \geq t_0$. Our third goal is to impose that the tracking error remains within some user-defined bounds, which adapt themselves according to some user-defined criteria. As an example, as a performance criterion, we design bounds on the tracking error to be such that if the control effort is low, then such bounds on the tracking error need to become tighter, since this condition implies that it is possible to enforce tighter constraints. Alternatively, if the control input approaches or exceeds its saturation limit, then such bounds on the tracking error must be relaxed. Finally, our last goal is that the closed-loop plant trajectory converges to the reference trajectory with a user-defined rate of convergence.

III. Two-Layer MRAC Systems

A classical limitation of MRAC is that the closed-loop plant trajectory reaches the reference trajectory as soon as or after the transient dynamics of the reference model has decayed, that is,

$$\alpha(e(\cdot)) \triangleq -\mathrm{Re}\left(\lambda_{\max}\left(A_{\mathrm{ref}}\right)\right),$$

where $\alpha(\cdot)$ captures the *rate of convergence* of its argument and $\lambda_{\max}(\cdot)$ denotes the eigenvalues of its argument with largest real part. Thus, the effort of tuning A_{ref}, which captures the transient behavior of the reference model, is lost for the most part [2], [9, Ch. 13].

Given the plant model (1) and the reference model (2), two-layer MRAC [2] ensures both uniform boundedness of the trajectory tracking error and of the adaptive gains and asymptotic convergence of the tracking error to zero, and allows to impose the rate of convergence on the tracking error. This result, which is detailed by the next theorem, is obtained without employing barrier functions, but by employing the control law

$$\phi(\pi, \hat{K}) = \hat{K}^{\mathrm{T}}\pi, \quad (\pi, \hat{K}) \in \mathbb{R}^{2n+m+N} \times \mathbb{R}^{(2n+m+N)\times m}, \tag{4}$$

where $\pi(t) \triangleq \left[\pi^{\mathrm{T}}(t), e^{\mathrm{T}}(t)\right]^{\mathrm{T}}$, the *adaptive gain* $\hat{K} : [t_0, \infty) \to \mathbb{R}^{(2n+m+N)\times m}$ verifies the *adaptive law*

$$\dot{\hat{K}}(t) = -\Gamma\pi(t)\varepsilon^{\mathrm{T}}PB, \quad \hat{K}(t_0) = \hat{K}_0, \quad t \geq t_0, \tag{5}$$

the adaptive rate matrix $\Gamma \in \mathbb{R}^{(2n+m+N)\times(2n+m+N)}$ is user-defined, symmetric, and positive-definite, $\varepsilon(t) \triangleq e(t) - e_{\mathrm{tran}}(t)$, $e_{\mathrm{tran}}(\cdot)$ is the solution of the *auxiliary reference model*

$$\dot{e}_{\mathrm{tran}}(t) = A_{\mathrm{tran}}e_{\mathrm{tran}}(t), \quad e_{\mathrm{tran}}(t_0) = e_{\mathrm{tran},0}, \quad t \geq t_0, \tag{6}$$

$A_{\mathrm{tran}} \in \mathbb{R}^{n\times n}$ is Hurwitz and user-defined, where $\mathrm{Re}\left(\lambda_{\max}\left(A_{\mathrm{tran}}\right)\right) < \mathrm{Re}\left(\lambda_{\min}\left(A_{\mathrm{ref}}\right)\right)$, $\lambda_{\min}(\cdot)$ denotes the eigenvalues of its argument with smallest real part, $P \in \mathbb{R}^{n\times n}$ denotes the symmetric, positive-definite solution of the *algebraic Lyapunov equation*

$$-Q = A_{\mathrm{tran}}^{\mathrm{T}} P + P A_{\mathrm{tran}}, \tag{7}$$

and $Q \in \mathbb{R}^{n\times n}$ is symmetric, positive-definite, and user-defined.

Theorem 1 ([2]): Consider the plant model (1), the reference model (2), the auxiliary model (6), and the adaptive law (5). If $u(t) = \phi(\pi(t), \hat{K}(t))$, $t \geq t_0$, where $\phi(\cdot,\cdot)$ is given by (4), then both $t \mapsto e(t)$ and $t \mapsto \hat{K}(t)$ are uniformly bounded on $[t_0, \infty)$, $\lim_{t\to\infty} e(t) = 0$ uniformly in $t_0 \in [0,\infty)$, and

$$\alpha(e(\cdot)) > -\mathrm{Re}\left(\lambda_{\min}\left(A_{\mathrm{ref}}\right)\right). \tag{8}$$

Equation (8) guarantees that the closed-loop plant trajectory $x(\cdot)$ reaches the reference trajectory $x_{\mathrm{ref}}(\cdot)$ before the transient dynamics of the reference model (2) has decayed. In classical MRAC, it holds that $\alpha(e(\cdot)) > -\mathrm{Re}\left(\lambda_{\min}\left(A_{\mathrm{ref}}\right)\right)$. The smaller is the real part of the eigenvalues of A_{tran} compared to the real part of the eigenvalues of A_{ref}, that is, the larger is $|\mathrm{Re}\left(\lambda_{\max}\left(A_{\mathrm{tran}}\right)\right) - \mathrm{Re}\left(\lambda_{\min}\left(A_{\mathrm{ref}}\right)\right)|$, the faster is the rate of convergence of the tracking error to zero.

IV. Funnel Two-Layer MRAC Systems

In this section, we build upon the two-layer MRAC architecture and allows to impose user-defined constraints. To state this result, let $\eta_{\max} > 0$ and $\overline{\eta} \in (0, \eta_{\max})$ be user-defined. Let the bounds on the trajectory tracking error be captured by the *constraint set*

$$\mathcal{E}_t \triangleq \left\{\varepsilon \in \mathbb{R}^n : H(t,\varepsilon) \geq 0\right\}, \qquad t \geq t_0, \tag{9}$$

where

$$H(t,\varepsilon) \triangleq \eta_{\max} - \eta^2(t) - \varepsilon^{\mathrm{T}} M \varepsilon, \quad (t,\varepsilon) \in [t_0,\infty) \times \mathbb{R}^n, \tag{10}$$

$M \in \mathbb{R}^{n\times n}$ is user-defined, symmetric, and nonnegative definite, and $\eta_{\max} - \eta^2(t)$ denotes the *diameter of the funnel* at time $t \geq t_0$. The function $\eta : [t_0,\infty) \to \mathbb{R}$ is such that the *adaptive law for the funnel diameter*

$$\dot{\eta}(t) = \begin{cases} \eta(t)\xi(t), \\ \quad \text{if } \varepsilon^{\mathrm{T}}(t) Q \varepsilon(t) \\ \quad\quad \geq 2V_e(t,\varepsilon(t))\eta^2(t)\xi(t) + \nu, \\ \quad\quad \text{and } \eta(t) \in \left[0, \sqrt{\overline{\eta} - \varepsilon^{\mathrm{T}}(t) M \varepsilon(t)}\right), \\ 0, \quad \text{otherwise} \end{cases}$$

$$\eta(t_0) = \eta_0, \quad t \geq t_0, \tag{11}$$

is verified, where $\eta_0 \in [0, \sqrt{\overline{\eta}})$, $\xi : [t_0,\infty) \to \mathbb{R}$ is continuous and user-defined, and $\nu > 0$ is user-defined. If $\eta_0 = 0$, then the diameter of the funnel will be equal to $\eta_{\max}$ for all $t \geq t_0$. The *barrier function* $V_e(\cdot,\cdot)$ in (11) is such that

$$V_e(t,\varepsilon) \triangleq \frac{\varepsilon^{\mathrm{T}} P \varepsilon}{H(t,\varepsilon)}, \quad (t,\varepsilon) \in [t_0,\infty) \times \mathring{\mathcal{E}}_t, \tag{12}$$

where $P \in \mathbb{R}^{n\times n}$ denotes the symmetric, positive-definite solution of (7) and $\mathring{\mathcal{E}}_t \triangleq \{\varepsilon \in \mathbb{R}^n : H(t,\varepsilon) > 0\}$ denotes the *interior* of $\mathcal{E}_t$.

It follows from (6) that $\lim_{t\to\infty} e_{\mathrm{tran}}(t) = 0$, and, hence, for $t \geq t_0$ sufficiently large, $\varepsilon(t)$ converges to $e(t)$. Thus, the constraint set (9) can be employed to effectively capture constraints on the tracking error $e(\cdot)$.

An example of function to regulate the diameter of the funnel is given by

$$\xi(t) = \frac{u_{\max} - \|u(t)\|}{\max\{\|u(t)\| - u_{\min}, \Delta u_{\min}\}}, \qquad t \geq t_0, \tag{13}$$

where $u_{\max} > u_{\min} \geq 0$ are user-defined and capture the upper and lower saturation constraints on the control input, respectively, and $\Delta u_{\min} > 0$ is user-defined. Note that the solution of (11) is given by

$$\eta(t) = \exp\left[\int_{t_0}^{t} \xi(\tau)\mathrm{d}\tau\right]\eta_0 \tag{14}$$

for all $t \geq t_0$ such that $\varepsilon^{\mathrm{T}}(t) Q \varepsilon(t) \geq 2V_e(t,\varepsilon(t))\eta^2(t)\xi(t) + \nu$ and $\eta(t) < \sqrt{\overline{\eta} - \varepsilon^{\mathrm{T}}(t) M \varepsilon(t)}$, and is constant otherwise. Therefore, (13) captures the requirement whereby the constraints on the trajectory tracking error given by (9) and (10) become tighter for $\|u(t)\|$ closer to $u_{\min}$ and looser for $\|u(t)\|$ closer to $u_{\max}$. Remarkably, (13) allows inverting the sign of $\dot{\eta}(\cdot)$ in the case $\|u(t)\| > u_{\max}$ for some $t \geq t_0$. Furthermore, the margin $\Delta u_{\min}$ should be chosen sufficiently small to allow reducing the diameter of the funnel as much as possible. However, overly small values of $\Delta u_{\min}$ may produce aggressive tightening of the funnel. In general, $\xi(\cdot)$ can be designed using any criteria or framework, such as feedback control theory or optimal control two name two.

Remark 4.1: The constraints captured by (10) are *hard* constraints, that is, inviolable constraints enforced by the control system at all times. The constraints enforceable through $\xi(\cdot)$ in (11), such as, for instance, (13) are *soft* constraints, that is, the proposed control system will attempt to enforce these constraints, which may be violated.

Finally, consider the control law (4) and the adaptive law

$$\dot{\hat{K}}(t) = -\Gamma H^{-1}(t,\varepsilon(t))\pi(t)\varepsilon^{\mathrm{T}}(t)\left[P + V_e(t,\varepsilon(t))M\right]B,$$

$$\hat{K}(t_0) = \hat{K}_0, \qquad t \geq t_0. \tag{15}$$

Theorem 2: Consider the plant model (1), the reference model (2), the adaptive law (15), the auxiliary model (6), and (11). If $e(t_0) \in \mathcal{E}_{t_0}$ and $u(t) = \phi(\pi(t), \hat{K}(t))$, $t \geq t_0$, where $\phi(\cdot,\cdot)$ is given by (4), then $e(t) \in \mathcal{E}_t$ for all $t \geq t_0$, both $t \mapsto \hat{K}(t)$ and $t \mapsto \eta(t)$ are uniformly bounded on $[t_0,\infty)$, and $\lim_{t\to\infty} e(t) = 0$ uniformly in $t_0 \in [0,\infty)$. Finally, (8) is verified.

Remark 4.2: In the application of Theorem 2, it is recommended to set

$$-\mathrm{Re}\left(\lambda_{\max}\left(A_{\mathrm{tran}}\right)\right) > \liminf_{t\to\infty} \frac{\int_{t_0}^{t} \xi(\tau)\mathrm{d}\tau}{t - t_0} \tag{16}$$

to assure that the rapid convergence of the tracking error to zero is due to the auxiliary model and the two-layer MRAC law and not of the converging funnel.

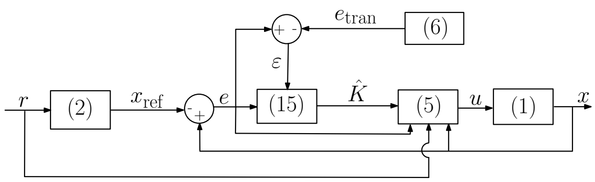

Fig. 1: Block diagram of the proposed MRAC system

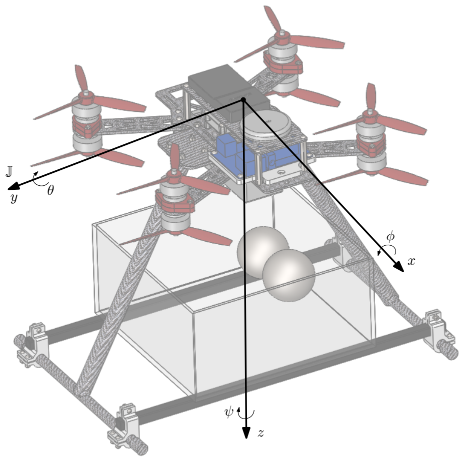

Fig. 2: CAD model of the X8-copter adopted in the numerical simulations with the payload

Figure 1 provides a schematic representation of the control algorithm that underlies Theorem 2.

V. Adaptive Control of An X8-Copter

To design the control architecture for an X8-copter UAV, such as the one shown in Figure 2, we recall that its translational dynamics are captured by

$$\dot{r}^{\mathbb{I}}(t) = v^{\mathbb{I}}(t), \qquad r^{\mathbb{I}}(t_0) = r_0^{\mathbb{I}}, \quad t \geq t_0, \tag{17a}$$

$$m\dot{v}^{\mathbb{I}}(t) = -R(\alpha(t))\Big[u_1(t)e_3 + \frac{1}{2}\rho_{\text{air}} S c_{\text{D}} \|v(t)\| v(t)\Big] + mge_3, \quad v^{\mathbb{I}}(t_0) = v_0^{\mathbb{I}}, \tag{17b}$$

where $r^{\mathbb{I}} : [t_0, \infty) \to \mathbb{R}^3$ denotes the position of the vehicle's center of mass in the inertial reference frame $\mathbb{I}$, $v^{\mathbb{I}} : [t_0, \infty) \to \mathbb{R}^3$ denotes the velocity of the vehicle center of mass in $\mathbb{I}$, $v(\cdot)$ denotes the UAV velocity expressed in the body reference frame $\mathbb{J}$, $m > 0$ denotes the mass of the UAV *without* payload, $\alpha(\cdot) \triangleq [\phi(\cdot), \theta(\cdot), \psi(\cdot)]^{\text{T}}$,

$$R(\alpha) \triangleq \begin{bmatrix} \text{c}\psi & -\text{s}\psi & 0 \\ \text{s}\psi & \text{c}\psi & 0 \\ 0 & 0 & 1 \end{bmatrix} \begin{bmatrix} \text{c}\theta & 0 & \text{s}\theta \\ 0 & 1 & 0 \\ -\text{s}\theta & 0 & \text{c}\theta \end{bmatrix} \begin{bmatrix} 1 & 0 & 0 \\ 0 & \text{c}\phi & -\text{s}\phi \\ 0 & \text{s}\phi & \text{c}\phi \end{bmatrix},$$

captures a rotation matrix, $\phi : [t_0, \infty) \to [0, 2\pi)$ $\theta : [t_0, \infty) \to (-\frac{\pi}{2}, \frac{\pi}{2})$, $\psi : [t_0, \infty) \to [0, 2\pi)$ denote the roll, pitch, and yaw angles of a 3-2-1 rotation sequence, respectively, $u_1 : [t_0, \infty) \to \mathbb{R}$ denotes the total thrust generated by the propellers, $g > 0$ denotes the gravitational acceleration, and $e_3 \triangleq [0, 0, 1]^{\text{T}}$. The air density $\rho_{\text{air}} > 0$, the UAV's cross-section area $S > 0$, and the diagonal, positive-definite drag coefficient matrix $c_{\text{D}} \in \mathbb{R}^{3\times 3}$ are unknown. The rotational dynamics are given by

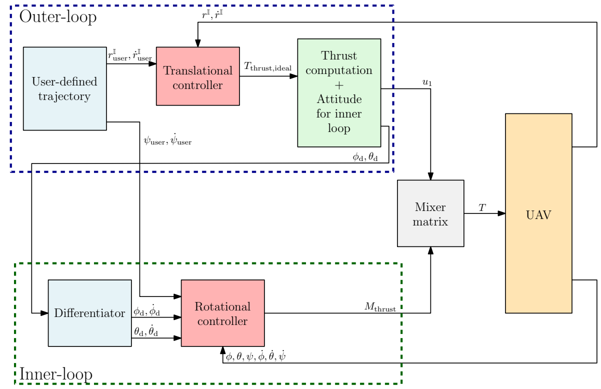

Fig. 3: Block diagram of the proposed control system for X8-copter

$$\dot{\alpha}(t) = \Gamma_{\text{J}}(\phi(t), \theta(t))\omega(t), \quad \alpha(t_0) = \alpha_0, \quad t \geq t_0, \tag{18a}$$

$$I\dot{\omega}(t) = \tau(t) - \omega^{\times}(t) I \omega(t), \quad \omega(t_0) = \omega_0, \tag{18b}$$

where $\omega : [t_0, \infty) \to \mathbb{R}^3$ denotes the *angular velocity* relative to an inertial reference frame,

$$\Gamma_{\text{J}}(\phi, \theta) \triangleq \begin{bmatrix} 1 & \sin\phi\tan\theta & \cos\phi\tan\theta \\ 0 & \cos\phi & -\sin\phi \\ 0 & \sin\phi\sec\theta & \cos\phi\sec\theta \end{bmatrix}, \tag{19}$$

$I = \text{diag}\left([I_x, I_y, I_z]\right)$ denotes the diagonal, positive-definite matrix of inertia with respect to the center of mass, and $\tau : [t_0, \infty) \to \mathbb{R}^3$ denotes the torque applied to the body. In this paper, if a vector $z \in \mathbb{R}^3$ is expressed in the reference frame $\mathbb{I}$, then it is denoted as $z^{\mathbb{I}}$. If $z \in \mathbb{R}^3$ is expressed in the reference frame $\mathbb{J}$, then it is denoted as z.

A. Outer loop design

To resolve the under-actuation of this UAV and determine the required total thrust, an outer loop is employed; see Figure 3. As detailed in [10], given the twice continuously differentiable user-defined reference trajectory $r_{\text{user}}^{\mathbb{I}} : [t_0, \infty) \to \mathbb{R}^3$ and a twice continuously differentiable desired yaw angle $\psi_{\text{user}} : [t_0, \infty) \to [0, 2\pi)$, to design the outer loop, we introduce the virtual translational control input $\mu^{\mathbb{I}} : [t_0, \infty) \to \mathbb{R}^3$ which can be designed applying an MRAC system so that the solution of

$$\dot{r}^{\mathbb{I}}(t) = v^{\mathbb{I}}(t), \qquad r^{\mathbb{I}}(t_0) = r_0^{\mathbb{I}}, \quad t \geq t_0, \tag{20a}$$

$$m\dot{v}^{\mathbb{I}}(t) = \mu^{\mathbb{I}}(t) - \frac{1}{2}\rho_{\text{air}} S R(\alpha(t)) c_{\text{D}} \|v(t)\| v(t) + mge_3, \quad v^{\mathbb{I}}(t_0) = v_0^{\mathbb{I}}, \tag{20b}$$

follows the user-defined trajectory $\left[r_{\text{user}}^{\text{T}}(t), \dot{r}_{\text{user}}^{\text{T}}(t)\right]^{\text{T}}$. Thus, a realization of the virtual control input is given by

$$\mu(t) = -u_1(t) R(\alpha_{\text{d}}(t)) e_3, \quad t \geq t_0, \tag{21}$$

where $\alpha_{\text{d}} : [t_0, \infty) \to [0, 2\pi) \times (-\frac{\pi}{2}, \frac{\pi}{2}) \times \{0\}$. The norm of $\mu(\cdot)$ determines the total thrust, and the orientation of

$\mu(\cdot)$ determines the desired roll angle $\phi_{\mathrm{d}} : [t_0, \infty) \to [0, 2\pi)$ and the desired pitch angle $\theta_{\mathrm{d}} : [t_0, \infty) \to (-\frac{\pi}{2}, \frac{\pi}{2})$ so that $\alpha_{\mathrm{d}}(t) \triangleq [\phi_{\mathrm{d}}(t), \theta_{\mathrm{d}}(t), 0]^{\mathrm{T}}$.

From (21), it follows that the components of $\mu^{\mathbb{I}}(\cdot)$ can be expressed as

$$\mu_X(t) = -u_1(t) \cos\phi_{\mathrm{d}}(t) \sin\theta_{\mathrm{d}}(t), \qquad t \geq t_0, \tag{22a}$$

$$\mu_Y(t) = u_1(t) \sin\phi_{\mathrm{d}}(t), \tag{22b}$$

$$\mu_Z(t) = -u_1(t) \cos\phi_{\mathrm{d}}(t) \cos\theta_{\mathrm{d}}(t). \tag{22c}$$

Hence, it follows from (22) that, for all $t \geq t_0$,

$$u_1(t) = \sqrt{\mu_X^2(t) + \mu_Y^2(t) + \mu_Z^2(t)}, \tag{23a}$$

$$\theta_{\mathrm{d}}(t) = \operatorname{atan2}(-\mu_X(t), -\mu_Z(t)), \tag{23b}$$

$$\phi_{\mathrm{d}}(t) = \operatorname{atan2}\left(\frac{\mu_Y(t)}{u_1(t)}, \sqrt{1 - \frac{\mu_Y^2(t)}{u_1^2(t)}}\right). \tag{23c}$$

The signed arc-tangent function allows accounting for the signs of its arguments and its codomain is $(-\pi, \pi]$. Equation (23) represent the output of the outer loop.

B. Inner loop design

The inner loop computes the moment of the thrust force $\tau(\cdot)$ needed to realize the desired attitude $[\phi_{\mathrm{d}}(t), \theta_{\mathrm{d}}(t), \psi_{\mathrm{user}}(t)]^{\mathrm{T}}$, $t \geq t_0$; see Figure 3. Since the rotational dynamics of a multi-rotor UAV are fully actuated, we can directly control the roll, pitch, and yaw angles with the three components of the torque $\tau(t) = [\tau_x(t), \tau_y(t), \tau_z(t)]^{\mathrm{T}}$, $t \geq t_0$. In this work, we let

$$\tau(t) = \omega^{\times}(t)\bar{I}\omega(t) + \bar{I}\tilde{\tau}(t), \qquad t \geq t_0. \tag{24}$$

where $\bar{I} \in \mathbb{R}^{3\times 3}$ denotes the estimated inertia matrix of the UAV computed with respect to the center of mass and $\tilde{\tau}(t) = [\tilde{\tau}_x(t), \tilde{\tau}_y(t), \tilde{\tau}_z(t)]^{\mathrm{T}}$. The first term on the right-hand side of (24) provides a baseline controller designed according to the dynamic inversion technique, which attempts to cancel the nonlinear term in (18b). The second term on the right-hand side of (24) can be designed employing an MRAC system so that

$$\lim_{t\to\infty} \|\alpha(t) - [\phi_{\mathrm{d}}(t), \theta_{\mathrm{d}}(t), \psi_{\mathrm{user}}(t)]^{\mathrm{T}}\| = 0$$

despite the fact that $\bar{I} \neq I$.

C. Thrust realization

Having deduced the total thrust $u_1(\cdot)$ and the moment of the thrust $\tau(\cdot)$, the final task is to compute how much thrust each motor of the X8-copter needs to produce. The relationship between total thrust, moment of the thrust, and thrust produced by each motor is given by

$$\begin{bmatrix} u_1(t) \\ \tau_x(t) \\ \tau_y(t) \\ \tau_z(t) \end{bmatrix} = \begin{bmatrix} 1 & l_y & -l_x & -c_T \\ 1 & l_y & l_x & c_T \\ 1 & -l_y & l_x & -c_T \\ 1 & -l_y & -l_x & c_T \\ 1 & l_y & -l_x & c_T \\ 1 & l_y & l_x & -c_T \\ 1 & -l_y & l_x & c_T \\ 1 & -l_y & -l_x & -c_T \end{bmatrix}^{\mathrm{T}} \begin{bmatrix} T_1(t) \\ T_2(t) \\ T_3(t) \\ T_4(t) \\ T_5(t) \\ T_6(t) \\ T_7(t) \\ T_8(t) \end{bmatrix}, \tag{25}$$

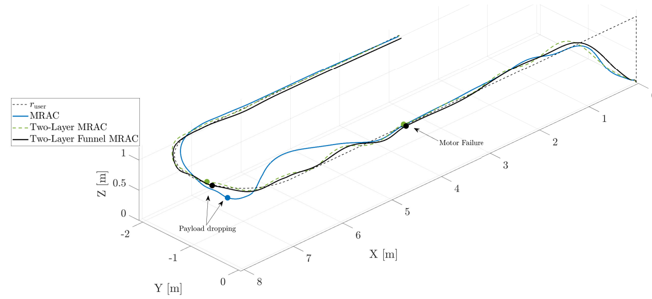

Fig. 4: Trajectories of the X8-copter in the mission devised for the numerical simulations. The plot shows where the UAV was at the time the motor failure and payload dropping happened, for each type of controller

where $l_x > 0$ denotes the distance between each motor and the pitch axis, $l_y > 0$ denotes the distance between each motor and the roll axis, $c_T > 0$ denotes the propellers' drag coefficient, and $T_i : [t_0, \infty) \to \mathbb{R}, i = 1, \ldots, 8$, denotes the thrust produced by motor i. Thus, we compute each motor's thrust force as

$$T(t) = M^{+}\left[u_1(t), \tau(t)\right]^{\mathrm{T}}, \qquad t \geq t_0, \tag{26}$$

where M^{+} denotes the *Moore-Penrose pseudoinverse* of the *mixer matrix* in (25) and $T(t) \triangleq [T_1(t), \ldots, T_8(t)]^{\mathrm{T}}$. Figure 3 shows the relationship between outer loop, inner loop, and thrust realization for an X8-copter.

VI. Numerical Simulations

In this section, we assess the performance of the proposed funnel two-layer MRAC system through high-fidelity numerical simulations executed in the high-fidelity environment PyChrono [8]. The UAV is tasked to follow a user-defined trajectory consisting of a 7 m straight segment, a sharp U-turn of 1 m radius, and an additional straight segment of 4 m at a constant altitude of 1.1 m. The user-defined translational velocity is 1.2 m/s, and it is requested that the UAV's roll axis is tangential to the user-defined trajectory at all times. At the intersection between the rectilinear and the semi-circular segments, the user-defined acceleration has an instantaneous variation of 1.44 m/s^2. An additional challenge lies in the fact that the UAV, whose mass is 2.025 kg, is transporting a payload inside its container, as shown in Figure 2, without being aware of it. The payload consists of two 0.539 kg steel balls having a radius of 0.0508 m that are free to move inside the container, hence the inertia properties of the vehicle vary substantially during flight. Furthermore, we consider the failure of two motors by setting $T_3(t) = 0$ and $T_8(t) = 0.5 \cdot T_{8,\mathrm{nominal}}(t)$ for all $t \geq 4$ s. The controllers are unaware of when the motors stop performing as expected. Additionally, after 7 s from the takeoff, the payload is unexpectedly dropped.

Figure 4 shows the trajectories followed by the X8-copter employing the results presented in Section IV, two-layer MRAC [2], and classical MRAC [9, Ch. 9]. Although all the control systems allow the UAV to complete its mission,

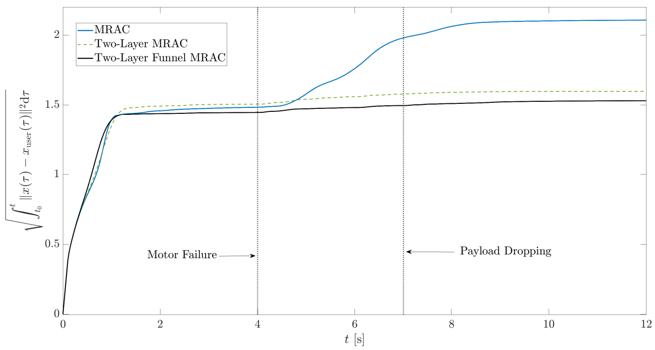

Fig. 5: $\mathcal{L}_2$-norm of the Euclidean norm of the trajectory tracking error.

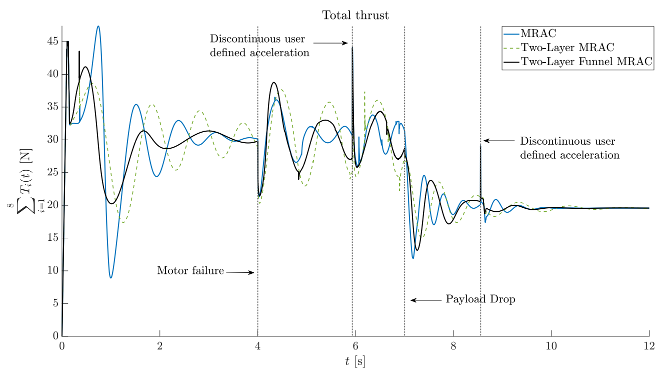

Fig. 6: Sum of the thrust forces exerted by each motor

the MRAC controller is the one suffering the most from the proposed challenges, especially the motor failure. It is worthwhile remarking that the tuning gains of the two-layer adaptive funnel MRAC system are the same as its classical counterpart, for fairness of comparison.

Figure 5 represents the $\mathcal{L}_2$-norm of the trajectory tracking error. The two-layer adaptive funnel MRAC system allows the trajectory tracking error to converge faster than any other techniques, and produces the smallest cumulative error.

Figure 6 shows the sum of the thrust forces generated by each motor. The thrust required by all control systems are substantially comparable. Remarkably, the funnel adaptive controller produce smaller oscillations in the thrust force than the classical two-layer MRAC system and the classical MRAC system. From these observations, we deduce that the two-layer adaptive funnel MRAC system allows improved trajectory tracking error at an effort that is similar to the effort required by the other controllers. A video of the proposed simulations is at [11].

VII. Conclusion

This paper presented a novel MRAC system, namely two-layer adaptive funnel MRAC. This system allows enforcing adaptive bounds on the trajectory tracking error presented in the form of a funnel. The diameter of the funnel can be designed to accommodate user-defined performance criteria. In this paper, as an example, the funnel was designed to allow soft constraints on the control effort. A unique feature of the two-layer adaptive funnel MRAC is that the rate of convergence of the trajectory tracking error can be enforced not by reducing the funnel diameter at a user-defined rate, but by introducing an additional reference model. An advantage of this approach is that enforcing convergence constraints by means of the barrier Lyapunov functions usually leads to more aggressive control inputs.

An extensive example shows the applicability and the advantages of the two-layer adaptive funnel MRAC. Specifically, we consider the problem of controlling an X8-copter tasked with transporting an unknown heavy payload along a user-defined trajectory. Additional challenges follow from unexpected motor faults, failures, and payload dropping. This example demonstrates how the proposed adaptive funnel control systems outperforms its classical counterparts.

Future work directions concern the analysis of multiple adaptive laws to regulate the funnel diameters. A relevant application of this work also concerns data-drive version of MRAC, such as those recently proposed in [12], where the tighter the region in which closed-loop trajectory is known to lie, the higher the efficiently of the control algorithm.

References

[1] T. Yucelen, G. D. L. Torre, and E. N. Johnson, "Improving transient performance of adaptive control architectures using frequency-limited system error dynamics," *International Journal of Control*, vol. 87, no. 11, pp. 2383–2397, 2014.

[2] R. B. Anderson, J. A. Marshall, and A. L'Afflitto, "Novel model reference adaptive control laws for improved transient dynamics and guaranteed saturation constraints," *Journal of the Franklin Institute*, vol. 358, no. 12, pp. 6281–6308, 2021.

[3] T. Berger, A. Ilchmann, and E. P. Ryan, "Funnel control of nonlinear systems," *Mathematics of Control, Signals, and Systems*, vol. 33, pp. 151–194, Mar 2021.

[4] B. M. Mirkin, "Decomposition-coordination optimization of the dynamic systems with adaptation of the criterion," *Automation and Remote Control*, vol. 62, pp. 1155–1164, Jul 2001.

[5] B. Mirkin, P.-O. Gutman, and J. Sjöberg, "Output-feedback MRAC with reference model tolerance of nonlinearly perturbed delayed plants," *IFAC Proceedings Volumes*, vol. 44, no. 1, pp. 6751–6756, 2011. IFAC World Congress.

[6] B. Mirkin, P.-O. Gutman, and Y. Shtessel, "Coordinated decentralized sliding mode MRAC with control cost optimization for a class of nonlinear systems," *Journal of the Franklin Institute*, vol. 349, no. 4, pp. 1364–1379, 2012. Special Issue on Optimal Sliding Mode Algorithms for Dynamic Systems.

[7] B. Mirkin and P.-O. Gutman, "Tube model reference adaptive control," *Automatica*, vol. 49, no. 4, pp. 1012–1018, 2013.

[8] Project Chrono, "Chrono: An Open Source Framework for the Physics-Based Simulation of Dynamic Systems." `https://projectchrono.org/`, 2014. Accessed: 2023-10-14.

[9] E. Lavretsky and K. Wise, *Robust and Adaptive Control: With Aerospace Applications*. London, UK: Springer, 2012.

[10] M. Gramuglia, G. M. Kumar, and A. L'Afflitto, "A hybrid model reference adaptive control system for multi-rotor unmanned aerial vehicles," in *SciTech*, (Orlando, FL), pp. 1–21, AIAA, 2024.

[11] M. Gramuglia, G. M. Kumar, and A. L'Afflitto, "Two-layer adaptive funnel mrac with applications to the control of multi-rotor uavs." `https://youtu.be/YFzCx4iFzpY`, 2024. Last accessed 02/20/2024.

[12] H. Wang, B. Scurlock, N. Powell, A. L'Afflitto, and A. J. Kurdila, "MRAC with adaptive uncertainty bounds via operator-valued reproducing kernels," *IEEE Control Systems Letters*, vol. 7, pp. 3771–3776, 2023.